Online measurement of factors influencing the electrostatic separation of mineral sands

by J.M. Lottering* and C. Aldrich*

Paper written on project work carried out in partial fulfilment of B Eng (Chem) degree

Synopsis

Operational factors influencing the electrostatic separation of mineral sands were investigated in a laboratory separator. Measurements were collected online by means of an optical sensor using diffused reflectance spectroscopy to determine the mineralogical composition. The results have shown that the roll speed and potential were the dominant operating variables, collectively explaining more than 83% and 68% of the product grade and yield, respectively. In contrast, the feed rate, temperature and position of the plate did not affect separation. The effect of the ambient relative humidity, ranging from 10% to 45%, could not be assessed conclusively and at best appeared to have a weakly beneficial effect on the product grade.

Keywords: process modelling, high tension roll separator, mineral sands

Background

Electrostatic separation of minerals is well established in the minerals industry, particularly with regard to the processing of beach sands and titaniferous alluvial deposits[1]. Despite the long-standing industrial use of high tension roll separators, the application of electrostatic separation technologies still faces major difficulties. Adequate control of operating variables, such as the potential, electrode configuration, roll speed, feed rate and temperature is vital to obtaining good results, while having to deal with disturbances such as ambient humidity and varying particle size distributions and compositions[2–3]. These variables behave interactively and minor adjustments to a single variable under certain mineral and atmospheric conditions can affect the performance of high tension roll separators considerably[4–5]. This incomplete understanding of machine operation has led to the evolvement of site-specific operating philosophies, making the electrostatic separation of mineral sands somewhat of a black art.

In this paper, the electrostatic separation of mineral sands is considered, but unlike previous experiments of a similar nature[6–7], separation was monitored online with an optical sensor, which allowed an analysis of the dynamics of electrostatic separation.

Experimental set-up

Experiments were conducted with a laboratory-scale Roche Mining Carrara high tension roll separator at the University of Stellenbosch, South Africa, as shown in Figure 1. The separator was fitted with a feed chute with electrical heating elements to allow the adjustment of the temperature of the feed. The speed of both feed and main roller drive motors, as well as the setting of the high tension voltage, were digitally controlled, while the position of the corona wire, high tension plate and splitter flaps on the discharge were all manually adjustable. Particles carried through the field generated by the corona wire electrode on the separation roller were electrically charged. A plate electrode attracted the conducting minerals, while the non-conducting particles remained on the roller surface. The plate electrode was angled to allow the conductor minerals to be pulled across the conductor splitter and into the conductor product chute. The non-conducting particles were brushed from the roller and directed into the non-conductor product chute. Although two separate middling products could be generated by a third splitter, the splitter plates were set up to produce only two exit streams. The feed was typical in size distribution and composition of that found on a heavy mineral separation plant.

* *Department of Process Engineering, University of Stellenbosch, Matieland, South Africa.*

 SA ISSN 0038–223X/3.00 + 0.00. Paper received Feb. 2006; revised paper received Mar. 2006.

The product mineralogy (non-conductor stream) was monitored online with Blue Cube Systems's MQi in-line mineral quantifier and the product mass flow was calculated by the difference between the feed mass flow and the conductor stream mass flow[8]. The online mineral quantifier uses diffused reflectance spectroscopy to determine the mineralogical composition of the mineral stream. It consisted of an optical scanning head, connected by optical fibre to an optics enclosure with an integrated dual-beam spectrometer and light source, in turn connected by multi-core cable to a data processor.

During operation the mineral sample was illuminated by a light source. A reflection probe in the scanning head detected reflected light from the passing mineral stream and an integrated spectrometer sensed the spectral distribution of the reflected light from the mineral particles, and transmitted the information to a data processor. The previously calibrated processor identified the spectral profiles of the different minerals in the sample being presented and accurately calculated the quantity of each mineral present with a maximum error of approximately 1%, as validated by manual grain counting. The results were displayed as a percentage of the total on a graphical user interface, while the output was also provided in the form of 4–20 mA signals suitable for input to SCADA or PLC systems. Both discharge streams were consequently combined and circulated in a continuous loop by a combination of vibration conveyors and a bucket elevator. The following operating variables were investigated.

- *Electrode potential (A)*—The gap between the corona wire and the roller determines the absolute voltage. Usually an increase in applied voltage gives a better quality of conductor product by increasing the recovery to the nonconductor product. However, an optimal voltage is generally reached where any further increase in applied voltage is irrelevant. Separation will therefore depend on the balance between the applied voltage and the roll speed.
- *Roll speed (B)*—Higher roll speeds increase recovery of conductors, but also decrease the quality. However, if too low a roll speed is used, the conductors tend to be entrained into the non-conductor product.
- *Feed rate (C)*—The feed rate could be varied by controlling the rotational speed of the feeder roll via the key pad of the variable speed drive. However, the actual feed rate is affected by the mineral composition and particle size of each sample. The variable speed drive could be adjusted in proportion to changes in the feed rate to dial achieve the desired feed rate from the actual feed rate. Moreover, the performance of the separator is affected at excessive feed rates. Under these conditions, conducting materials that are trapped among non-conductors tend to dislodge the non-conductors, causing them to end up in the middling or conductor products.
- *Position of the corona wire electrode (D)*—Setting the corona wire at a 60 mm gap at the top dead centre of the roll and applying a voltage of 26 kV will generally give good separation. This could be accomplished by loosening the external locking handle on the apparatus and adjusting the gap between the roller and the corona wire or by rotating the insulated wire support bar to precisely position the wire as required between the feed point and the plate electrode.

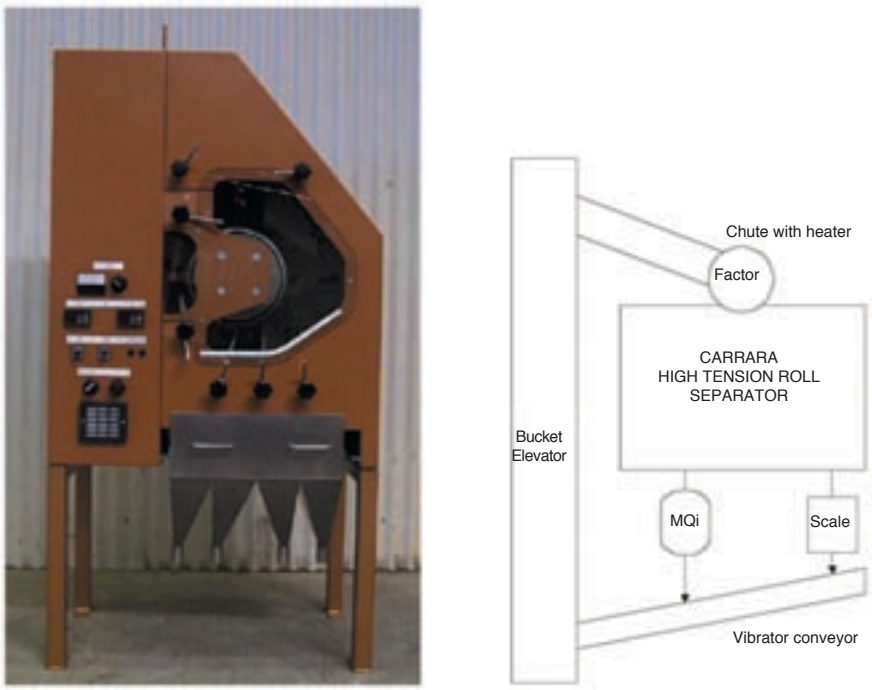

Figure 1—(a) The Roche Mining Carrara Laboratory High Tension Roll Separator, and (b) a diagrammatic representation of the main components of the separator

- *Position of the plate electrode (E)*—The electrode plate is responsible for discharging the various particles. The rate of discharge is affected by the position of the plate, and the more conductive the feedstock, the wider the plate gap should be for best separation.
- *Temperature (F)*—The temperature, has among other, an effect on the humidity and therefore also has a potential influence on the electrode charge, as well as an effect on the conductivity of the minerals.

A fractional factorial design was used to determine which of the factors (A–F) discussed above had the greatest effect on the grade and product yield. Only two levels were considered for each of the six operating variables or factors and $2^{6-1} = 32$ runs (i.e. a half fraction) were initially done. With this resolution VI design, each main effect is aliased with a single 5-factor interaction and each 2nd order interaction is aliased with a single 4-factor interaction. All main effects and 2nd order interactions could therefore also be estimated, based on the assumption that the higher order interactions were negligible.

Results

Product grade and yield

The details of the runs, as well as the results are summarized in Table I. All values, except for that of the position of the plate and the wire, were measured online and these results shown are the average values over a period of five minutes.

From the ANOVA results summarized in Table II, it is clear that the model is significant (F = 12.47) and that factors A (19.9%), B (48.3%) and D, (4.56%) could explain most of the variance in the grade. Likewise, the interaction between factors A and B, as well as B and D, was also significant, explaining approximately 14.7% and 4.24% of the variance in the grade, respectively. The observed dominance of the electrode potential (factor A) and roll speed (factor B) is consistent with the results of previous authors[4,6].

A similar analysis was done with the yield as dependent variable, where the same variables and interactions were found to be dominant (Table III). In this case factors A, B and D explained 20.8%, 32.2% and 7.13% of the variance of the yield, while the 2nd order interactions AB and BD, respectively, explained 15.1% and 8.19% of the variance of the yield.

Additional centre point runs were consequently run to construct an optimized model of the grade and yield as functions of A, B and D. The results of these experiments are indicated in Table IV.

A distance-weighted least squares method was used to fit a response surface to the data in Tables I and IV, i.e. at each point in the data set a 2nd degree polynomial was fitted to a subset of the data around the point whose response was being estimated. With weighted least squares more weight is given to points near the point whose response is being estimated and less weight to points further away. The value

Table I

Grade and yield in % zircon at specific operating conditions

Std	Run	A: Electrode potential (kV)	B: Roll speed (Hz)	C: Feed speed (Hz)	D: Wire position (-)	E: Plate position (-)	F: Temperature (°C)	Grade (% zircon)	Yield (% zircon)
1	5	15	30	30	-1	-1	30	87.56	97.32
2	22	21	30	30	-1	-1	50	87.25	93.98
3	8	15	55	30	-1	-1	50	92.42	80.84
4	16	21	55	30	-1	-1	30	88.21	93.70
5	17	15	30	50	-1	-1	50	88.02	97.16
6	18	21	30	50	-1	-1	30	87.96	98.09
7	10	15	55	50	-1	-1	30	95.33	59.97
8	32	21	55	50	-1	-1	50	88.84	95.53
9	31	15	30	30	1	-1	50	87.81	94.17
10	19	21	30	30	1	-1	30	86.72	100
11	15	15	55	30	1	-1	30	99.92	27.96
12	7	21	55	30	1	-1	50	91.61	88.64
13	3	15	30	50	1	-1	30	88.61	91.72
14	28	21	30	50	1	-1	50	87.81	96.93
15	21	15	55	50	1	-1	50	99.13	44.21
16	4	21	55	50	1	-1	30	93.14	78.77
17	6	15	30	30	-1	1	50	87.83	94.75
18	27	21	30	30	-1	1	30	86.82	100
19	14	15	55	30	-1	1	30	94.08	84.96
20	11	21	55	30	-1	1	50	88.43	95.08
21	20	15	30	50	-1	1	30	87.42	97.19
22	26	21	30	50	-1	1	50	87.83	97.86
23	29	15	55	50	-1	1	50	93.33	84.08
24	9	21	55	50	-1	1	30	88.89	95.86
25	2	15	30	30	1	1	30	87.15	100
26	30	21	30	30	1	1	50	87.84	95.10
27	23	15	55	30	1	1	50	96.07	37.76
28	13	21	55	30	1	1	30	88.81	100
29	12	15	30	50	1	1	50	88.36	97.93
30	1	21	30	50	1	1	30	86.88	100
31	25	15	55	50	1	1	30	96.02	41.54
32	24	21	55	50	1	1	50	89.53	88.44

Table II

ANOVA of product grade (the bold entries in the last column indicate contributions significant at a P < 0.01 level)

Grade						
Source	**SS**	**df**	**MS**	**F**	**P**	**% Contrib**
(A) KV	86.2	1	86.2	102.553	0.000	**19.90**
(B) Roll	209.4	1	209.4	248.984	0.000	**48.32**
(C) Feed	2.2738	1	2.2738	2.704	0.128	0.52
(D) Wire	19.8	1	19.8	23.508	0.001	**4.56**
(E) Plate	7.1159	1	7.1159	8.463	0.014	1.64
(F) Temp.	0.0657	1	0.0657	0.078	0.785	0.02
AB	63.7	1	63.7	75.762	0.000	**14.70**
AC	0.1070	1	0.1070	0.127	0.728	0.02
AD	2.4920	1	2.4920	2.964	0.113	0.58
AE	0.1339	1	0.1339	0.159	0.697	0.03
AF	0.7412	1	0.7412	0.881	0.368	0.17
BC	0.0195	1	0.0195	0.023	0.882	0.00
BD	18.4	1	18.4	21.855	0.001	**4.24**
BE	4.3439	1	4.3439	5.166	0.044	1.00
BF	2.3274	1	2.3274	2.768	0.124	0.54
CD	0.0639	1	0.0639	0.076	0.788	0.01
CE	1.1514	1	1.1514	1.369	0.267	0.27
CF	0.0570	1	0.0570	0.068	0.799	0.01
DE	5.3546	1	5.3546	6.368	0.028	1.24
DF	0.3342	1	0.3342	0.397	0.541	0.08
Model	324.84	6	54.14	12.47	< 0.0001	
Error	9.249	11	0.841			2.13
Total	433.27	31				

Table III

ANOVA of product yield (the bold entries in the last column indicate contributions significant at a P < 0.01 level)

Yield						
Source	**SS**	**df**	**MS**	**F**	**P**	**% Contrib**
(A) KV	2787.6	1	2787.6	34.922	0.000	**20.82**
(B) Roll	4311.7	1	4311.7	54.015	0.000	**32.20**
(C) Feed	33.3	1	33.3	0.417	0.532	0.25
(D) Wire	954.7	1	954.7	11.960	0.005	**7.13**
(E) Plate	201.0	1	201.0	2.517	0.141	1.50
(F) Temp.	0.6244	1	0.6244	0.008	0.931	0.00
AB	2016.0	1	2016.0	25.255	0.000	**15.06**
AC	9.1699	1	9.1699	0.115	0.741	0.07
AD	608.7	1	608.7	7.626	0.019	4.55
AE	9.1699	1	9.1699	0.115	0.741	0.07
AF	102.8	1	102.8	1.288	0.281	0.77
BC	4.2705	1	4.2705	0.053	0.821	0.03
BD	1096.9	1	1096.9	13.741	0.003	**8.19**
BE	48.2	1	48.2	0.604	0.454	0.36
BF	131.4	1	131.4	1.646	0.226	0.98
CD	2.2952	1	2.2952	0.029	0.868	0.02
CE	1.5444	1	1.5444	0.019	0.892	0.01
CF	181.9	1	181.9	2.279	0.159	1.36
DE	0.1755	1	0.1755	0.002	0.963	0.00
DF	9.4721	1	9.4721	0.119	0.737	0.07
Model	8289.0	6	1381	6.772	0.000237	
Error	878.07	11	79.824			6.56
Total	13389	31				

Table IV

Grade and yield in % zircon at specific centre point factors

Std	Run	A: Electrode potential (kV)	B: roll speed (Hz)	C: Feed speed (Hz)	D: Wir position (-)	E: Plate position (-)	F: Temperature (°C)	Grade (% zircon)	Yield (% zircon)
33	43	18	43	40	0.5	0.5	40	86.87	99.77
34	36	18	43	40	0.5	0.5	40	87.00	97.2
35	34	18	43	40	0.5	0.5	40	86.84	96.82
36	40	18	43	40	0.5	1	40	88.02	100
37	39	18	43	40	0.5	0	40	87.95	100
38	33	18	43	40	1	0.5	40	87.96	98.16
39	42	18	43	40	0	0.5	40	87.62	100
40	37	18	55	40	0.5	0.5	40	89.19	94.09
41	35	18	30	40	0.5	0.5	40	87.11	100
42	38	21	43	40	0.5	0.5	40	87.06	100
43	41	15	43	40	0.5	0.5	40	87.80	95.25

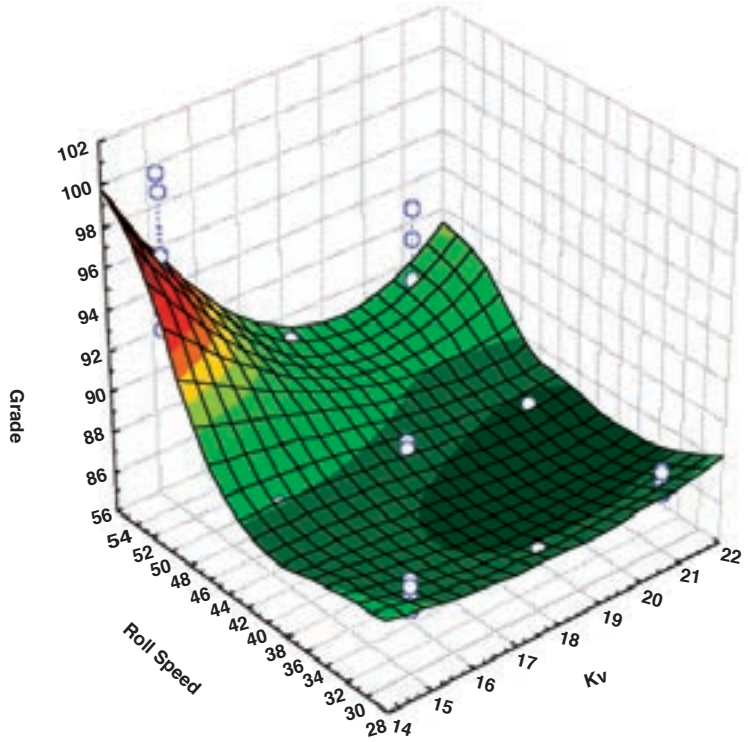

Figure 2—Effect of roll speed and potential on product grade

of the regression function for the point is then obtained by evaluating the local polynomial using the explanatory variable values for that data point[9].

The results are shown in Figures 2 and 3 for the grade and product yield, respectively. The experimental data are indicated by circular markers on these response surfaces showing the effect of roll speed and potential. The models explained more than 83% and 68% of the variance in the grade and yield, respectively. As indicated in Figures 2 and 3, the maximum grade is obtained at a high roll speed and a low potential, while the maximum yield is obtained a high roll speed and a high potential.

Ambient humidity

The effect of ambient humidity on electrostatic separation is complex in that it can affect the conductivity of the air and hence the charging of the particles, as well as the conductivity of the particles[10]. Figure 4 shows the relationship between humidity measurements and the temperature, while Figure 5 shows the relationship between the relative humidity measurements and the grade, after accounting for the roll speed, potential, and wire position on the product grade. Some weakly nonlinear correlation may be present, with an increase in humidity having a slightly beneficial effect on the grade, but this needs to be confirmed by more appropriate experiments.

Dynamics of electrostatic separation

With the spectral sensor, grades and yields could be calculated online, collecting a sample approximately every

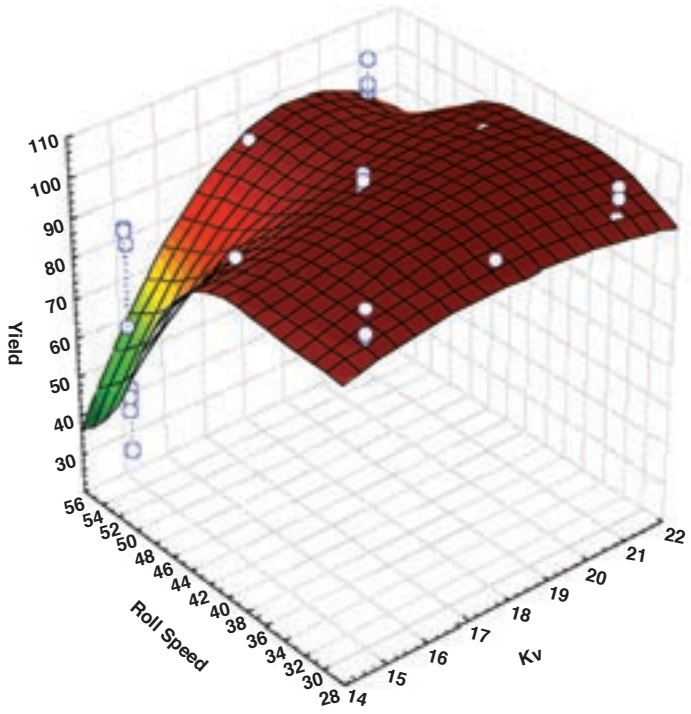

Figure 3—Effect of roll speed and potential on product yield

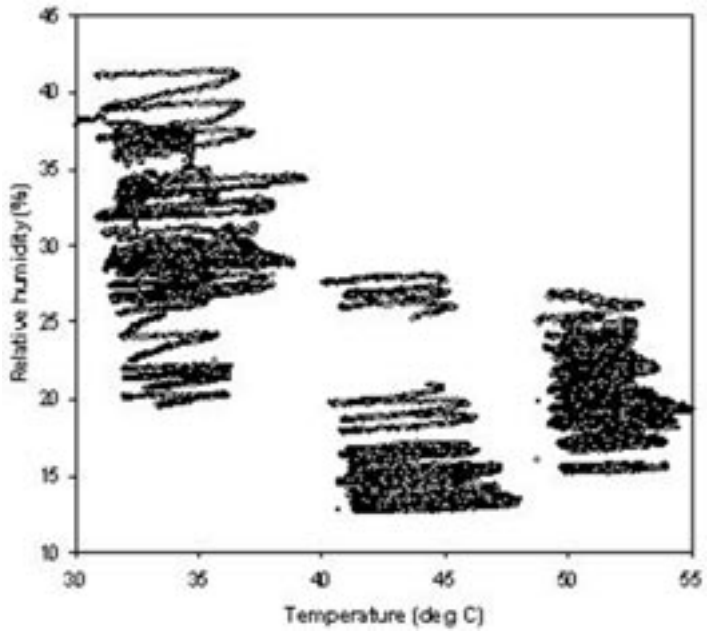

Figure 4—Relationship between temperature and relative humidity

100 ms. For example, Figure 6 shows the product grade measurements associated with Run 2 (nominally 30 Hz, as in Table I). In this figure, the measurements are shown in the top left panel, estimated the autocorrelation function of the measured data in the bottom left panel, and lag plots of the data in the panels on the right-hand side.

In Figure 6, the lag plots were constructed from the product grade data, which could be presented generically as a time series of length n = 438 (Equation [1])

$$y = [y_0, y_1 \ldots y_{n-1}]^T \qquad [1]$$

This series was used to construct a trajectory matrix ($Z \in \Re^{KxL}$) of the data (Equation [2]), so that

$$\mathbf{Z} = \begin{bmatrix} y_0 & y_1 & \cdots & y_{L-1} \\ y_1 & y_2 & \cdots & y_L \\ \mathrm{M} & \mathrm{M} & \mathrm{O} & \mathrm{M} \\ y_{K-1} & y_K & \cdots & y_{n-1} \end{bmatrix} \qquad [2]$$

Useful information about the dynamics of the observed system can be obtained from a principal component analysis of this trajectory matrix, i.e. by decomposing matrix Z as indicated below (Equation [3]).

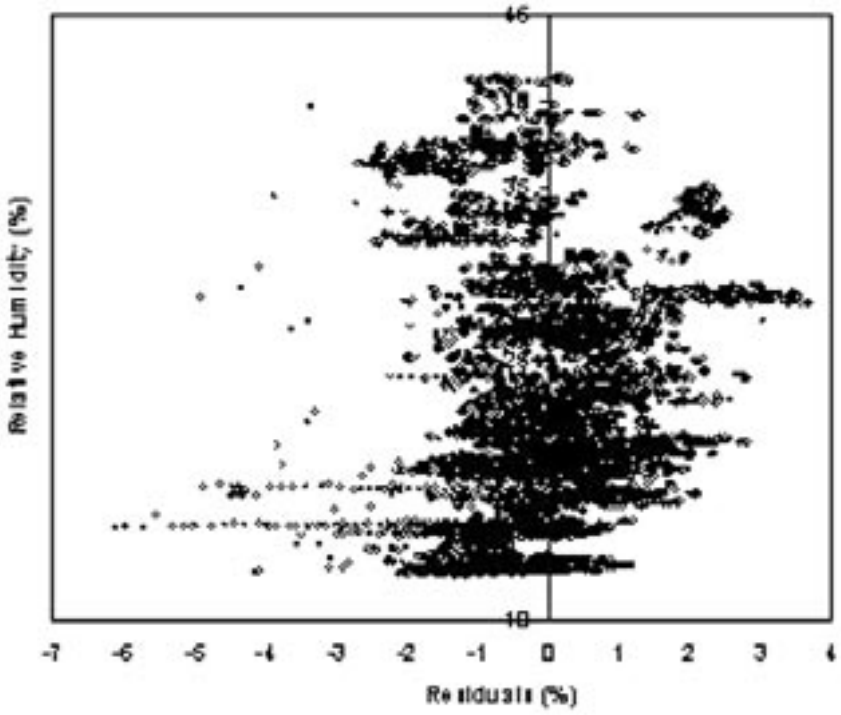

Figure 5—Relationship between relative humidity and product grade, after accounting for the roll speed and potential

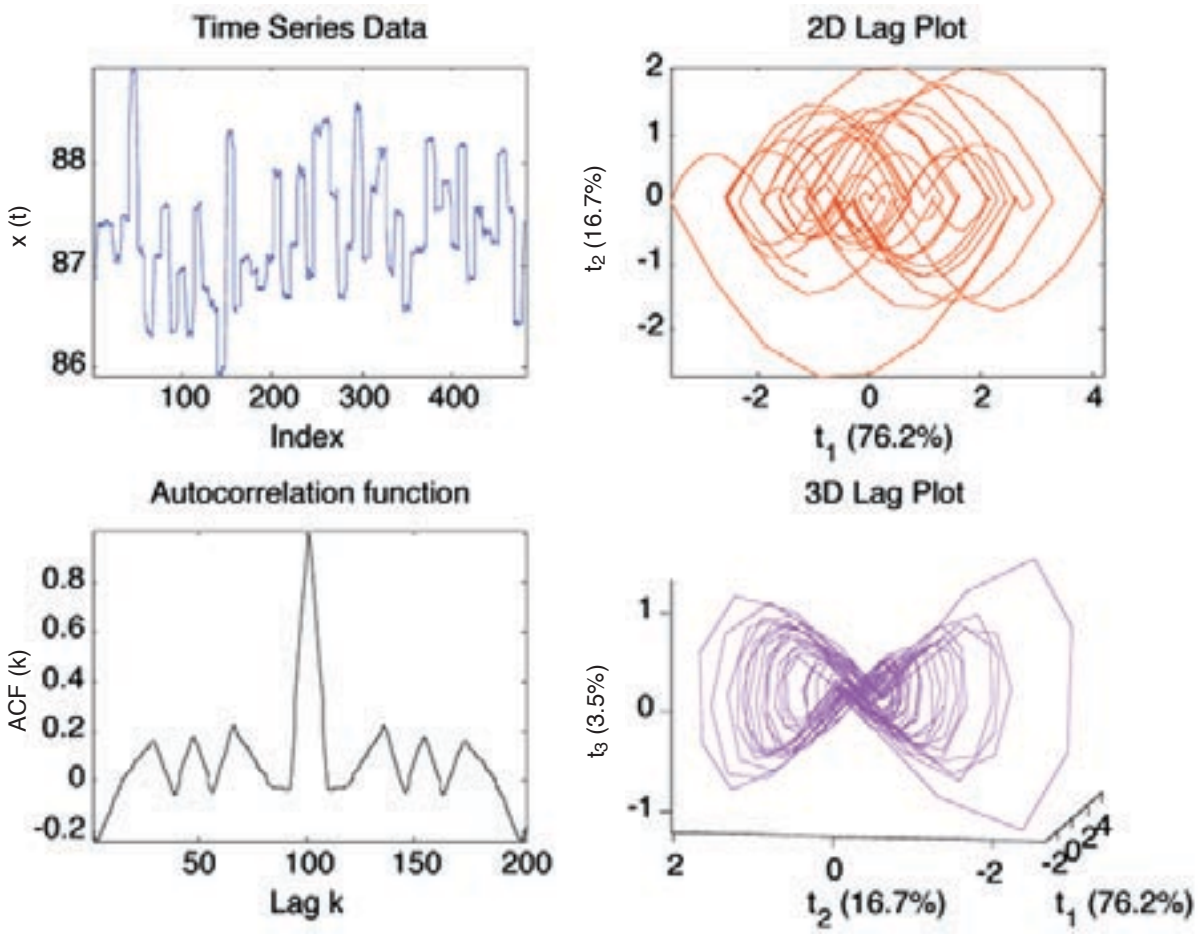

Figure 6—Actual grade measurements for Run 2 (top, left), estimated autocorrelation function of time series data (bottom, left), 2D and 3D lag plots of the data (top, right and bottom right, respectivley)

$$Z = t_1 p_1^T + t_2 p_2^T + \ldots t_{L-1} p_{L-1}^T \quad [3]$$

The right-hand panel in Figure 6 shows plots of the first two and the first three score vectors (t_1, t_2 and t_3). The values of the variables as measured did not fluctuate randomly, but exhibit remarkably well-defined periodic behaviour, as indicated in Figures 6, for Run 2. These remarkably regular orbits are a likely artefact of the operation of the equipment and appeared to be related to the switching behaviour of the thermostat on the separator. Note that the oscillations were small at any rate, ranging from approximately 86% to 89% for the grade (Run 2). Removal of the oscillatory trend yielded a signal that could be represented by an autoregressive model (not shown here).

As a consequence, further work will have to be done to assess the feasibility of the development of advanced process control systems (typically depending on reliable process models), particularly as far as larger-scale industrial systems are concerned.

Discussion and conclusions

Measurements of the product yield and grade were affected by the operation of the equipment. When the separator operated continuously for long periods of time, particles were observed to leave the rotor and land on the conductor chute, probably owing to small charges building up on these particles. This may also have been the reason for the particles observed to sticking to the metal chute, instead of sliding along it and into the mass flow scale. When too many particles got stuck on the chute, the whole bed of particles tended to avalanche along the chute and enter the mass flow scale simultaneously. This caused the mass flow scale to operate incorrectly and inaccurately, affecting the yield calculation.

Likewise, the mass flow scale was not particularly sensitive and it did not operate correctly when very small amounts of the conductor particles flowed through it. Moreover, the scale was located near the vibrating conveyor and was therefore affected by vibration. As a result, the yield was often calculated as more than 100% at certain settings.

The initial 'high' setting for the roller speed and 'low' setting for the high voltage was 70 Hz and 13 kV, respectively. However, it was found that at these settings a significant amount of the non-conducting particles ended up in the conductor chute, thus flooding the mass flow scale, again making the yield calculations less accurate. In contrast, at very low settings of the roller speed, the centrifugal force was insufficiently small and as a result the conductor particles were not able to overcome the pinning force initiated by the corona wire. These conductor particles ended up in the non-conductor chute, making for poor separation.

If the high voltage setting of the corona wire electrode was too high, the surface charge of the particles induced by the corona wire electrode was so large that even the conducting particles picked up a pinning force that outweighed all other forces needed for the particle to separate from the rotor. Again, these conductor particles ended up in the non-conductor chute, making for poor separation. Also, at potential settings in excess of 21 kV, the potential difference between the corona wire and the rotor surface was so high that the wire arced onto the rotor. Low settings of the wire position increased the probability of this occurring, causing the software used to control the high tension roll separator to terminate operation, so that the run had to be repeated.

These experimental issues notwithstanding, the results have shown that

- The roll speed and potential had a dominant influence on the product grade and yield, explaining approximately 83% of the variance of the product grade, and 68% of the product yield. In contrast, the feed rate and temperature did not affect separation.
- Over the range of 10%–45%, the ambient relative humidity appeared at best to have a weak effect on separation.
- Most of the process variables, as well as the quality variables, could be measured accurately online by making use of a proprietary optical sensor, with a maximum error of approximately 1%.
- The dynamics of the process, as measured in terms of the quality variables (product and grade) could be described adequately by an autoregressive process, once some oscillatory behaviour likely to be an artefact of the equipment had been removed.

Acknowledgements

The authors are grateful to Blue Cube Systems (Pty) Ltd in Stellenbosch, who have made their experimental rig, as well as their online mineral sensor available for the project.

References

1. Celik, M.S. and Yaser, E. Effect of temperature and impurities on electrostatic separation of boon minerals, *Minerals Engineering*, vol. 8, no. 7, 1995. pp. 829–833.
2. Kelly, E.G. and Spottiswood, D.J. The theory of electrostatic separation: A review, Part I: Fundamentals, *Minerals Engineering*, vol. 2, no. 1, 1989. pp. 33–46.
3. Kelly, E.G. and Spottiswood, D.J. The theory of electrostatic separation: A review, Part II: Particle charging, *Minerals Engineering*, vol. 2, no. 2, 1989. pp. 193–205.
4. Dance, A.D. and Morrison, R.D. Quantifying a Black Art: The electrostatic separation of mineral sands, *Minerals Engineering*, vol. 5, no. 7, 1992. pp. 751–756.
5. Aman, F. and Morar, R. High-voltage electrode position: A key factor of electrostatic separation efficiency, *IEEE Transaction on Industry Application*, vol. 40, no. 3, 2004. pp. 905–910.
6. Dascalescu, L., Tilmatine, A., Aman, F., and Mihailescu, M. Optimization of electrostatic separation process using response surface modeling, *IEEE Transactions on Industry Applications,* vol. 40, no. 1, 2004. pp. 53–59.
7. Mihailescu, M., Samuila, A., Urs, A., Morar, R., Iuga, A., and Dascalescu, L. Computer-assisted experimental design for optimization of electrostatic separation processes, *IEEE Transactions on Industrial Applications*, vol. 38, 2002. pp. 1174–1181.
8. De Waal, P. and Du Plessis, F.E. Automatic control of a high tension roll separator, *Heavy Minerals 2005*, Society for Mining, Metallurgy and Exploration, 2005.
9. McLain, D.H. Drawing contours from arbitrary data points, *Computer Journal*, vol. 17, 1974. pp. 318–324.
10. Kelly, E.G. and Spottiswood, D.J. The theory of electrostatic separation: A review, Part III: The separation of particles, *Minerals Engineering*, vol. 2, no. 3, 1989. pp. 337–349.